Equation of State, Thermal Expansion Coefficient, and Isothermal Compressibility for Ices Ih, II, III, V, and VI, as Obtained from Computer Simulation†

E. G. Noya,* C. Menduiña, J. L. Aragones, and C. Vega

Departamento de Química Física, Facultad de Ciencias Químicas, Universidad Complutense de Madrid, 28040 Madrid, Spain

Received: June 4, 2007

A relatively simple equation of state is proposed for several forms of ice, whose parameters have been fitted to the results of extensive computer simulations using the TIP4P/Ice and TIP4P/2005 models of water. Comparison with available experimental data for ice Ih shows that both models reproduce the experimental density and isothermal compressibility to good accuracy over the entire range of thermodynamic stability except at low temperatures. The predictions for the thermal expansion coefficient are slightly worse but still reasonable. Results obtained with the TIP4P/2005 model are slightly better than those obtained with the TIP4P/Ice model. At temperatures below 150 K, the predictions of both models deviate significantly from experiment. As expected, at low temperatures, quantum effects become increasingly important, and classical simulations are unable to accurately describe the properties of ices. In fact, neither the heat capacity nor the thermal expansion coefficient go to zero at zero temperature (as they should be according to the third law of thermodynamics). Predicted compressibilites are however reliable even up to 0 K. Finally, the relative energies of the ices at 0 K have also been estimated and compared with the experiments.

I. Introduction

Water is an essential molecule. In the liquid phase, water presents a number of anomalies when compared to other liquids.[1−4] In the solid phase, it exhibits one of the most complex phase diagrams, having 15 different solid structures. Of these 15 solid structures, 9 of them are thermodynamically stable, and the other 6 (Ic, IV, IX, XII, XIII, and XIV) are metastable. Due to its importance and its complexity, understanding the properties of water from a molecular point of view is of considerable interest. The experimental study of the phase diagram of water has spanned the entire 20th century, starting with the pioneering work of Tammann and Bridgman[5,6] up to the recent discovery of ices XII, XIII, and XIV.[7,8] The existence of several types of amorphous phases at low temperatures, [9−11] the possible existence of a liquid−liquid phase transition in water,[12,13] and the properties of ice at a free surface[14] have also been the focus of much interest in the last two decades.

Water is also challenging from a theoretical point of view. The first computer simulations of water were performed by Barker and Watts[15] and by Rahman and Stillinger[16] in the early 1970s. In the most popular models,[17] water is treated classically, often as a rigid nonpolarizable molecule, with the positive charge located on the hydrogen atoms and a Lennard-Jones (LJ) interaction site located on the oxygen atom. Differences appear in the location of the negative charge. When the negative charge is located on the oxygen atom, one has the family of models with three interaction sites formed by TIP3P,[18] SPC,[19] and SPC/E.[20] When the negative charge is located on the H−O−H bisector, the model has four interaction sites, as in the case of TIP4P.[18] When the negative charge is located on the "lone-pair electrons", one has a model with five interaction sites, as with TIP5P.[21] Computer simulation studies of water have focused mainly on the liquid phase. Although some preliminary results for ice Ih were published in 1972,[22] the first NVT simulations were not performed until a few years later. The number of simulation studies devoted to the solid phases of water is by far smaller than the number of simulation studies devoted to the liquid properties. Early work by Morse and Rice[23] showed clearly that the old potential models of the 1970s do not correctly describe the densities of the ices. Further work on the equation of state (EOS) of the ices has been performed in the last years.[24−33]

Taking into account the importance of water and the question of whether the current models of water can be used to describe the solid phases (ices) or even to predict the phase diagram, a systematic study has been undertaken by our group in the last 3 years.[34−40] We have found that TIP3P, SPC, SPC/E, and TIP5P yield a bad prediction of the phase diagram of water.[34,41] In fact, for these models, ice II was more stable than ice Ih at normal pressure, and besides, ices III and V were not stable phases for these models. Moreover, the melting points predicted by these models were quite low (with the only exception of TIP5P).[40] With respect to their ability to reproduce the densities of the different solid polymorphs, it has been found that SPC/E and TIP5P overestimate the density of ices by about 3 and 8%,[34,39] respectively (the performance of TIP3P and SPC has not been tested yet).

The failure of these models is in contrast with the success of the TIP4P model.[18,42] In fact, the TIP4P model is able to predict reasonably well the phase diagram of water.[34] It predicts ice Ih as the stable solid phase at the normal melting point. The prediction of the densities for the different solid phases of water appears as reasonable (it overestimates the experimental densities by about 2%).[39] The main failure of the model seems to be a melting point about 40 K below the experimental value.[34,43] In view of these results, it was more or less obvious that the parameters of the TIP4P model could be modified slightly to yield improved performance. It is with this idea in mind that

† Part of the "Keith E. Gubbins Festschrift".

10.1021/jp0743121 CCC: $37.00
Published on Web 10/03/2007

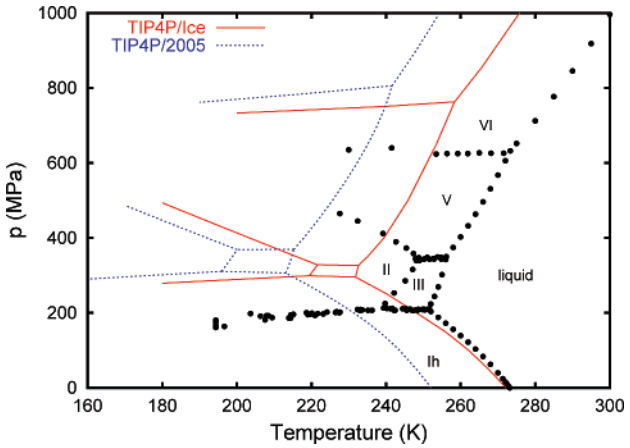

Figure 1. Phase diagram of the TIP4P/2005 and TIP4P/Ice models, together with the experimental phase diagram (stars).

the TIP4P/Ew[44] and TIP4P/2005[45] models have recently been proposed. These two models reproduce quite nicely one of the fingerprint properties of water, the maximum in density of water at room pressure. A new model, known as the TIP4P/Ice,[46] has also been proposed and has been found to reproduce the experimental melting temperature of water. The impossibility of simultaneously reproducing the temperature of maximum density and the melting point for nonpolarizable models has been shown recently.[47]

Besides providing good phase diagrams, the two new models, TIP4P/Ice and TIP4P/2005, predict quite well the densities of the different polymorphs of water, having the typical deviation with respect to the experiment of about −1% for TIP4P/Ice[46] and of about 1% for TIP4P/2005.[45] When considering the deviation between experiment and simulation results for each model, one single thermodynamic state was selected for each solid phase.[45,46] For this reason, although the performance of TIP4P/Ice and TIP4P/2005 for these selected states was good, a more extensive comparison between simulation and experimental results is needed to assess the performance of these models over a broad range of thermodynamic conditions. This is especially interesting, taking into account the renewed interest in determining experimentally the equation of state of the different solid phases of water. As an example of this, Feistel and Wagner have recently proposed an equation of state for ice Ih which is valid over the whole range of thermodynamic stability and whose parameters have been fitted to a selection of the most reliable experimental data.[48] For other high-pressure polymorphs, such as ices II, III, and V, equations of state have been proposed by Tchijov and co-workers.[49,50] However, since experimental data are not as abundant for these ices as those for ice Ih, these authors generated an equation of state by generalizing the method proposed by Fei et al.[51] In this method, it is only necessary to know the specific volume along some isotherm and some isobar. Moreover, when there was not enough experimental data, Tchijov and co-workers used a combination of experimental[52,53] and simulation[24,54] results.

In this work, extensive simulations have been performed for the different solid phases of water using the TIP4P/Ice and TIP4P/2005 models. There are three main goals of this paper. The first one is to provide an extensive comparison between simulation and experiment in a broad range of thermodynamic conditions to check the performance of the models. Second, the determination of the EOS in a broad range of thermodynamic states allows determination of some interesting properties, such as the isothermal compressibility and the coefficient of thermal expansion. It would be of interest to compare the predictions of the models with the experimental results (where available). Moreover, since for many solid phases of water these coefficients have not yet been measured, the results of the simulations provide at least an estimate of the magnitude. Third, another interesting issue is the presence of quantum effects in water and particularly in the solid phases of water. It is expected that models such as those used here, when treated classically, will fail in predicting the properties of ices at low temperatures. Although this is obvious, it would be of interest to determine at which temperatures the classical description fails completely in the estimation of the properties of the solid phases of water.

TABLE 1: Parameters of the Potential Models

model	ϵ/k (K)	Σ (Å)	q_H (e)	d_{OM} (Å)
TIP4P	78.0	3.154	0.520	0.150
TIP4P/Ice	116.1	3.1688	0.5897	0.1577
TIP4P/2005	93.2	3.1589	0.5564	0.1546

The structure of the paper is as follows. The model and simulation details are described in section II. In section IIIA, the simulation results will be presented, and an EOS describing the simulation data reasonably well will be proposed. A comparison of the proposed equations of state with experimental results will be made in section IIIB. In section IIIC, the results for several thermodynamic coefficients (isothermal compressibility, coefficient of thermal expansion) will be presented. In section IIID, the radial distribution function of ice Ih will be given and compared to experiments. In section IIIE, we will revise the experimental data used in previous studies to assess the performance of the TIP4P/Ice[46] and TIP4P/2005 models.[45] Moreover, the properties at zero temperature and pressure will be discussed and compared with experiments in section IIIF. Finally, the main conclusions of this work will be summarized in section IV.

II. Simulation Details

The two model potentials used in this work are the TIP4P/Ice and TIP4P/2005 models. The parameters of the original TIP4P model and their modified counterparts are presented in Table 1. As can be seen in the table, the main differences between TIP4P and TIP4P/Ice are a larger value of the charge located on the H atoms and a larger value of the dispersion energy of the LJ interaction site. The parameters of the TIP4P/2005 are just between those of TIP4P and TIP4P/Ice. The melting points of the TIP4P, TIP4P/2005, and TIP4P/Ice models are 230,[31,34,35,55] 250,[43,45,56] and 272 K,[43,46,56] respectively. In Figure 1, the experimental phase diagram of water is compared to the predictions of TIP4P/2005 and TIP4P/Ice. These two models describe qualitatively the phase diagram of water quite well.

NpT Monte Carlo (MC) simulations have been performed for the following solid structures of water: ice Ih, II, III, V, and VI. The simulations were performed both for the TIP4P/Ice and for the TIP4P/2005 model. For each ice, about 50 different thermodynamic states were considered. The selected states were chosen within the region of the experimental phase diagram where the solid phases are thermodynamically stable. In the simulations described in this work, the LJ potential was truncated at 8.5 Å for all of the phases. Standard long-range corrections were added to the LJ energy. Ewald sums were used to deal with the long-range electrostatic forces. The real part of the electrostatic contribution was also truncated at 8.5 Å. The screening parameter and the number of vectors of reciprocal space considered had to be carefully selected for each crystal

phase.[57,58] The number of molecules used for ice Ih, II, III, V, and VI was 288, 432, 324, 504, and 360, respectively. These system sizes guarantee that the smallest edge of the simulation box is always larger than twice the cutoff in the potential.

Since the considered solid structures are not cubic Ih (hexagonal), II (trigonal), III and VI (tetragonal), and V (monoclinic), anisotropic NpT MC simulations (Parrinello−Rahman-like[59,60]) were necessary for the solid phases, thus allowing both the shape and the relative dimensions of the unit cell to change. Typically, about 80000 cycles were undertaken for the determination of the properties of each state (a cycle is defined as a trial move per particle plus a trial volume change). These properties were calculated after a 20000 cycle equilibration period. For the proton disordered phases (Ih and VI), the algorithm of Buch et al.[61] was used to generate an initial configuration having no net dipole moment, where the hydrogens (but not the oxygens) are disordered and satisfy the ice rules.[42,62] The remaining disordered phases, ice III and ice V, required some additional care, as they are known to exhibit only partial disorder.[63] In view of this, the algorithm given in ref 61 was generalized[36] to construct an initial configuration with biased occupation of the hydrogen positions. Ice II presents no proton disorder; thus, crystallographic information was used to generate an initial solid configuration.[64] The atom−atom correlation functions (O−O, H−H, and O−H) were evaluated every 5 cycles. The width of the grid used to compute $g(r)$ was on the order of 0.05 Å. Correlation functions were evaluated up to 7.5 Å.

Before leaving this section, we would like to make a comment. For each solid phase, the selected thermodynamic states were chosen within the "region of the phase diagram where this solid is thermodynamically stable in the experimental phase diagram". However, as shown in Figure 1, the region where, say, ice II is thermodynamically stable in the experimental phase diagram is not identical to the region where ice II is thermodynamically stable for the, say, TIP4P/2005 model.[45] Therefore, in certain cases, we will perform simulations of ice II (a similar problem arises for other solid phases) under conditions where ice II is not thermodynamically stable for the considered water model. This may cast some doubts on the validity of our results. We would like to stress that it is easy to perform simulations of ice II at thermodynamic states where it is not thermodynamically stable, as long as it remains mechanically stable. In fact, we found that, for the TIP4P/Ice and TIP4P/2005 models, the region where they remain mechanically stable is, by far, larger than the region where they are thermodynamically stable. Moreover, we have never found solid−solid transitions taking place directly in our NpT simulations. The only possible transformation of the solid within NpT simulations when taken outside of the region of the phase diagram where it is thermodynamically stable is the melting to a liquid. However, we have shown that spontaneous melting under periodic boundary conditions without a free surface occurs typically at temperatures about 90 K above the true melting point[65] (superheating has also been experimentally observed for ice Ih, although it occurred only over a short time scale[66]). Therefore, at room pressure, it is possible to perform simulations of ice Ih using the TIP4P/Ice model up to temperatures of about 330 K without observing melting, even though the thermodynamic melting point for this model (where the chemical potential of the liquid and solid becomes identical) occurs at 272 K. In the same way, it is possible to simulate ice Ih at 273 K for a model such as TIP4P/2005 that exhibits a melting point of 252 K. In summary, the ice phases have about 90 K of additional mechanical stability with respect to melting, and besides, they show an extraordinary resistance to undergo solid−solid transformations by the application of pressure (at least for the lengths of the runs considered in this work).

III. Results and Discussion

A. Proposed Equation of State. In order to construct an EOS, we have to start by choosing a functional form for the density that will depend both on the temperature and on the pressure and that will contain a small number of parameters. The values of these parameters will then be obtained from a fit to the results of our simulations. The function that we propose is based on the Murnaghan equation of state, which accounts for the dependence of the volume on pressure at constant temperature[67]

$$\rho(p) = \rho_0\left(1 + B_0' \frac{p}{B_0}\right)^{1/B_0'} \tag{1}$$

Here, ρ_0 is the equilibrium density at the reference pressure, and B_0 and B_0' are the parameters of a linear fit to the variation of the bulk modulus (B) with pressure

$$B = \rho\left(\frac{\partial p}{\partial \rho}\right) \tag{2}$$

$$= B_0 + B_0' p \tag{3}$$

In order to introduce the dependence on temperature, we modified this equation of state in such a way that the density ρ_0 depends on the temperature and the quotient B_0'/B_0 depends both on the pressure and on the temperature. Therefore, the final expression can be written as

$$\rho(p) = (c_1 + c_2 T + c_3 T^2 + c_4 T^3) \times (1 + (p - p_0)(c_5 + c_6 p + c_7 T + c_8 T^2))^{c_9} \tag{4}$$

where the c_i are the adjustable parameters. The reference pressure p_0 is chosen as the lowest pressure at which our simulations have been carried out for each ice. The c_i parameters have been fitted to reproduce the results of MC simulations performed with the TIP4P/Ice and TIP4P/2005 models.

The tables with all of the raw data from the simulations are provided as Supporting Information. Besides the results within the region of thermodynamic stability, we have included also as Supporting Information the results for the densities and energies along the isotherm $T = 100$ K for ices Ih, II, III, V, and VI. The reason why data along the isotherm $T = 100$ K have also been included is because experiments aimed to predict the structure of ice polymorphs are usually performed around 100 K, and therefore, the simulation results could be useful to compare with such experiments. In addition, the radial distribution functions at some selected states are also provided. In particular, we have chosen to provide the radial function for each phase at two states. One state within the region of thermodynamic stability of each phase and the other at 77 K and at room pressure.

The parameters resulting from the fit to the simulation data for each of the studied ices are shown in Table 2. The root-mean-square deviation was typically on the order of 10^{-3} (in g cm^{-3}). Note that, as our EOS has been fitted to simulation results within the region of thermodynamic stability of each ice phase as measured in experiments, the fit should not be used outside of this region. In the caption to Table 2, the range of validity of the fit for each phase is given.

TABLE 2: Parameters of the Equation of State (eq 4) for Ices Ih, II, III, V, and VI Obtained from a Fit to the MC Simulation Data Using the TIP4P/Ice and TIP4P/2005 Model Potentials[a]

	Ih		II	
	TIP4P/Ice	TIP4P/2005	TIP4P/Ice	TIP4P/2005
c_1	0.9333645563931860	0.9523508411749246	1.162380521111319	1.144338224524182
c_2	$-1.6538763925959943\times10^{-5}$	$-7.7401559795826369\times10^{-5}$	$6.4339104419833220\times10^{-4}$	$1.2226599111716179\times10^{-3}$
c_3	$-4.9131710735359650\times10^{-7}$	$-2.6344907230534274\times10^{-7}$	$-4.2853736285872941\times10^{-6}$	$-7.4363819197860952\times10^{-6}$
c_4	$6.8574635779667510\times10^{-10}$	$2.7954298907267541\times10^{-10}$	$6.6366781037355693\times10^{-9}$	$1.1930409942943458\times10^{-8}$
c_5	$-8.0022573040769078\times10^{-5}$	$-1.5115876478694266\times10^{-4}$	$5.1775617109126904\times10^{-5}$	$4.4761612901132599\times10^{-5}$
c_6	$5.5827889012324885\times10^{-9}$	$2.1071736158073251\times10^{-8}$	$3.0565575291423941\times10^{-10}$	$1.9496445704192729\times10^{-10}$
c_7	$-2.3799623887981696\times10^{-8}$	$-1.5964810641973470\times10^{-7}$	$-1.2771511724094005\times10^{-7}$	$-4.3225649249182538\times10^{-8}$
c_8	$-4.1763417991812277\times10^{-10}$	$-3.6555620029379607\times10^{-10}$	$5.5728021296251606\times10^{-10}$	$3.7028546874689732\times10^{-10}$
c_9	$7.5464396748841640\times10^{-2}$	$4.5329345462526041\times10^{-2}$	0.1134341595259877	0.1216992426011108
p_0	0	0	1500	1500

	III		V	
	TIP4P/Ice	TIP4P/2005	TIP4P/Ice	TIP4P/2005
c_1	0.7901120280281187	0.7867033369676349	0.9578251754575851	1.125399314320533
c_2	$2.0610879892472296\times10^{-3}$	$2.1083273684731334\times10^{-3}$	$1.8592645030336193\times10^{-3}$	$1.2848360323428980\times10^{-3}$
c_3	$1.8336044693291669\times10^{-6}$	$1.9996061925830519\times10^{-6}$	$-2.8789245931810953\times10^{-7}$	$-2.9827434815990351\times10^{-6}$
c_4	$-1.7957882078134850\times10^{-8}$	$-1.8403846353793885\times10^{-8}$	$-1.0830223107096555\times10^{-8}$	$-7.0240647830805534\times10^{-10}$
c_5	$1.1833799359721640\times10^{-4}$	$-9.4219965130986978\times10^{-4}$	$2.8408267014116193\times10^{-2}$	$1.5387562174445470\times10^{-3}$
c_6	$2.7486204201299804\times10^{-9}$	$8.6550581794603172\times10^{-7}$	$9.5050287451069000\times10^{-8}$	$1.2274049292906057\times10^{-10}$
c_7	$-1.8048013597969550\times10^{-6}$	$-6.2939386737083316\times10^{-6}$	$-2.2892819879510626\times10^{-4}$	$-1.1701030122362814\times10^{-5}$
c_8	$7.0474227637629241\times10^{-9}$	$2.3776274301095990\times10^{-8}$	$4.6164780649162607\times10^{-7}$	$2.3781092398594965\times10^{-8}$
c_9	0.1029147782598036	$1.2058493936096935\times10^{-2}$	$1.4773795318967098\times10^{-2}$	$6.7677348798317087\times10^{-2}$
p_0	2200	2200	3500	3500

	VI	
	TIP4P/Ice	TIP4P/2005
c_1	1.399854365472994	1.420781210754346
c_2	$-2.2620511234175047\times10^{-4}$	$-1.8767767786597854\times10^{-4}$
c_3	$-6.4445905460312822\times10^{-9}$	$-3.0277732428240016\times10^{-7}$
c_4	$-3.7356226146631561\times10^{-10}$	$-4.3307679778853911\times10^{-11}$
c_5	$2.6009917818679855\times10^{-5}$	$2.9942638850346679\times10^{-5}$
c_6	$2.8824030542638774\times10^{-11}$	$2.3171920382045466\times10^{-10}$
c_7	$-4.7445181322000103\times10^{-9}$	$9.4242295662052573\times10^{-9}$
c_8	$1.1828599537024005\times10^{-10}$	$1.6169196558781717\times10^{-10}$
c_9	0.1272545208763955	0.1032847803405029
p_0	8000	8000

[a] The p_0 Is given in bars, temperature in K, and the density, as obtained from eq 4, is given in g cm^{-3}. These EOSs are only valid within the region of thermodynamic stability of each phase, at $p = 1-2000$ bar and $T = 100-273.15$ K for ice Ih, $p = 1500-6500$ bar and $T = 160-240$ K for ice II, $p = 2200-3400$ bar and $T = 240-254$ K for ice III, $p = 3500-6000$ bar and $T = 220-270$ K for ice V, and $p = 8000-20000$ Bars and $T = 175-325$ K for ice VI. Equation 4 should not be used outside of the range of the validity of the fit.

B. Comparison of the Proposed EOS with Experiments. We will start by discussing the results for ice Ih. This is the ice for which more experimental data are available, and the comparison of our results with these experimental data will allow us to assess the reliability of the simulations and of the model potentials. Most of these experimental data, which include measurements of several thermodynamic properties of ice Ih, have been collected and revised by Feistel and Wagner.[48] Besides, these authors proposed an equation of state for ice Ih that was fitted to a selection of the more accurate of these measurements.[48] Therefore, a comparison of our EOS (based on simulation data) with the EOS of Feistel and Wagner (based on the experimental data and which will be named as FW EOS) will serve to test the validity of our EOS over the whole range of thermodynamic stability.

Figure 2 shows the temperature dependence of the density at different pressures $p = 1$, 1000 and 2000 bar for ice Ih. In this figure, we have plotted the data obtained from the TIP4P/Ice and TIP4P/2005 EOSs (eq 4), as well as the corresponding values obtained from the FW EOS.[48] At high temperatures, the agreement between the simulations and the FW EOS is fairly good over the whole range of pressures. In general, the TIP4P/2005 model shows better agreement with the FW EOS at temperatures close to room temperature (the differences are on the order of 0.1−0.2%). However, none of the models exhibits a bending in the curve of the density that leads to a smaller dependence of the density with temperature in the low-temperature region, as observed in the FW EOS that reproduces the experimental results. We will see later that these qualitative differences between simulations and experiments are even more pronounced at temperatures below $T = 100$ K. From this analysis, it can be inferred that both models reproduce the experiments quite accurately at temperatures above $T = 150$ K, the TIP4P/2005 model giving slightly better results than those of the TIP4P/Ice.

We also compared our results for ice Ih with some recent experimental data performed by Strässle et al.[68] that had not been included in the study of Feistel and Wagner.[48] By means of neutron diffraction, these authors determined the equation of state of D_2O ice at $T = 145$ K for high pressures. Assuming that the unit cell is not effected by the change of the hydrogen isotope, these experimental results are also valid for H_2O. Figure 3 shows these experimental measurements, as well as the densities provided by the TIP4P/Ice, TIP4P/2005, and FW EOSs in the range of $p = 0-2000$ bar. The first thing to note in Figure 3 is that the experimental FW EOS is able to predict the experimental results of Strässle et al. quite accurately, the differences being on the order of 0.3%. On the other hand, the

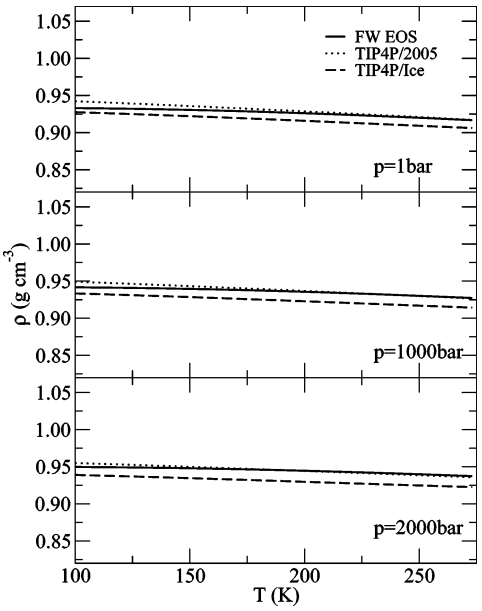

Figure 2. Density (ρ) for ice Ih at $p = 1$, 1000, and 2000 bar, predicted by the TIP4P/2005 and TIP4P/Ice models. For comparison, data obtained used the experimental FW EOS are also shown.

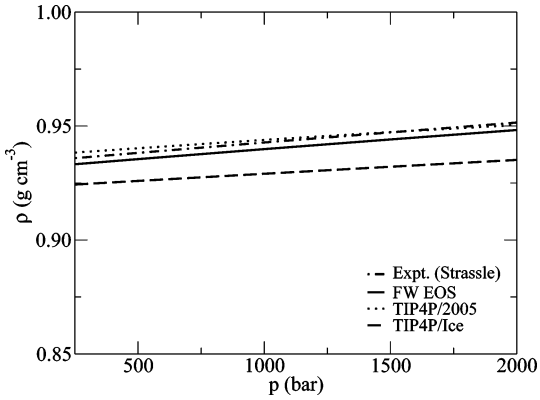

Figure 3. Comparison of the variation of the density of ice Ih with pressure at $T = 145$ K predicted by the TIP4P/2005 and TIP4P/Ice models with experimental data of Strässle et al.[68] For comparison, the FW EOS is also shown.[48]

densities obtained from our EOS fitted to the TIP4P/Ice and TIP4P/2005 simulations are also in fairly good agreement with the results of Strässle et al., the TIP4P/2005 model again giving the more accurate results (0.1−0.3 versus 1.0−1.2% with the TIP4P/Ice).

In order to study in more detail the discrepancies found at low temperatures, we also performed some simulations below $T = 100$ K. Figure 4 and Table 3 show that the differences with experiments become more dramatic as we move to lower temperatures. The simulations predict that the density continues to increase as the temperature decreases, in clear disagreement with the experimental results, where it has been seen that the density achieves an almost constant value from a temperature of approximately 100 to 0 K. The experimental behavior of the density at lower temperatures is imposed by the third law of thermodynamics. A consequence of this principle is that the cubic thermal expansion α, that is, the derivative of the volume with respect to the temperature, must go to 0 at 0 K.[69] However, the results of the simulations violate this condition. The density increases with decreasing temperature, even at very low temperatures approaching $T = 0$ K, and therefore, the cubic expansion coefficient will not vanish at 0 K. These discrepancies

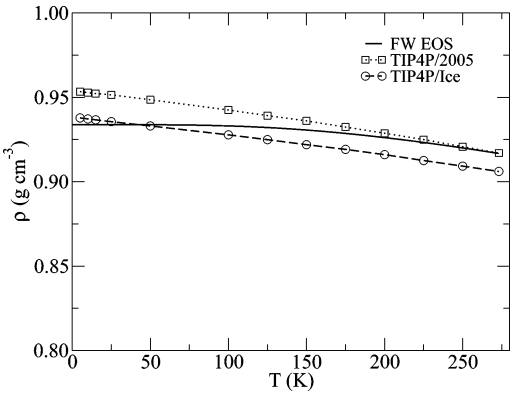

Figure 4. Temperature dependence of the density of ice Ih at $p = 1$ bar predicted by the TIP4P/2005 and TIP4P/Ice models as compared to the FW EOS.[48] At low temperatures, the deviation is more pronounced.

TABLE 3: Variation of the Density of Ice Ih with Temperature at $p = 1$ bar as Obtained from Simulations Using the TIP4P/2005 and TIP4P/Ice Models, Together with the FW EOS[48] Which is Based on Experimental Results; for the TIP4P/2005 Model, the Difference between the Simulation Result and the FW EOS ($\Delta\rho = \rho_{TIP4P/2005} - \rho_{FW}$) for Each of Thermodynamic State is also Shown

	ρ (g cm^{-3})			
T (K)	expt.	TIP4P/2005	$\Delta\rho$	TIP4P/Ice
5	0.9338	0.9533	0.0195	0.9378
25	0.9338	0.9514	0.0176	0.9356
50	0.9337	0.9486	0.0149	0.9330
100	0.9330	0.9425	0.0095	0.9277
150	0.9306	0.9360	0.0054	0.9219
200	0.9261	0.9287	0.0026	0.9160
250	0.9200	0.9207	0.0007	0.9092
273	0.9167	0.9170	0.0003	0.9061

are due to the fact that we performed classical MC simulations, and it is well-known that quantum corrections must be taken into account at low temperatures.[70−72] Even though it was expected that classical simulations would fail at low temperatures, our results show up to what temperatures they are reliable. As Figure 4 shows, at room pressure, a classical treatment gives reasonable results at temperatures above $T = 150$ K, while quantum simulations (i.e., path integral simulations) must be performed at lower temperatures.

The deviation of simulations from experiments for the isobar $p = 1$ bar as a function of temperature has been calculated (see $\Delta\rho = \rho_{TIP4P/2005} - \rho_{FW}$ in Table 3). In particular, the deviations $\Delta\rho$ as a function of temperature can be fitted to a fourth degree polynomial of the form

$$\Delta\rho = a + bT + cT^2 + dT^3 + eT^4 \qquad (5)$$

where T is given in Kelvin, $\Delta\rho$ in g cm^{-3}, and the values of the parameters (in the corresponding units) are $a = 0.02001660403$, $b = -9.203263521 \times 10^{-5}$, $c = -3.489274256 \times 10^{-7}$, $d = 2.725676965 \times 10^{-9}$, and $e = -4.340802725 \times 10^{-12}$. Therefore, an empirical correction (which accounts for quantum effects) to the TIP4P/2005 model simulations can be obtained from this expression. It can probably also be used for other ices at room pressure as a rough estimate.

For the rest of the ices, experimental data are much more scarce. There has been only a few experimental groups that have performed measurements of the equation of state for ices II, III, V, and VI. In particular, for D_2O, there are some measurements of the compressibility at $T = 225$ K and of the thermal expansion at normal pressure for ice II by Fortes et al.[73] For

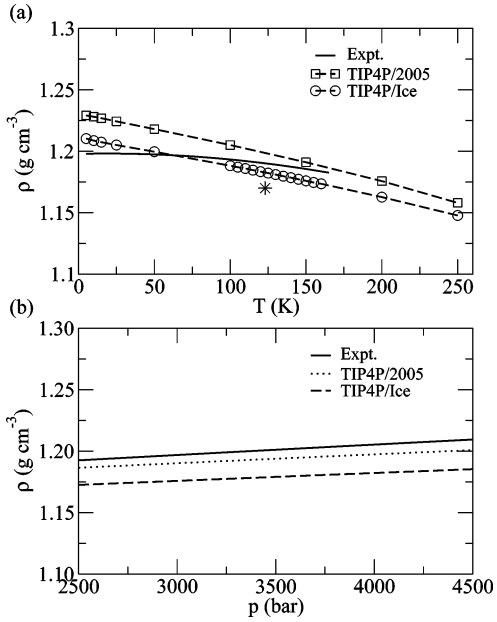

Figure 5. Comparison of (a) the temperature dependence of the density of ice II at room pressure and (b) the pressure dependence of the density of ice II at $T = 225$ K predicted by the TIP4P/2005 and TIP4P/Ice models with experimental data reported by Fortes et al.[73] In (a), the experimental datum of Kamb[75] (asterisk) has also been included for comparison (see discussion in Section IIIE).

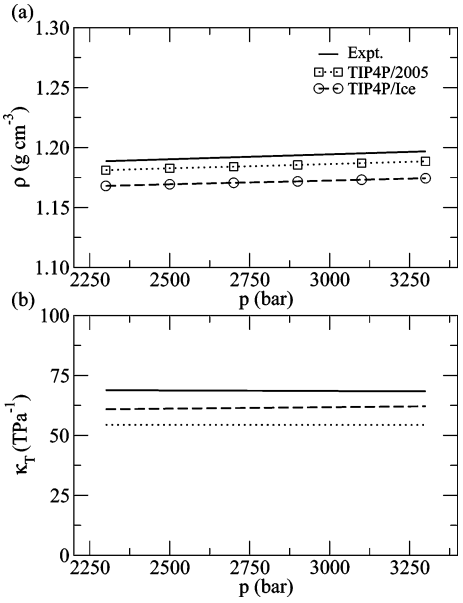

Figure 6. Comparison of (a) the temperature dependence of the density of ice II and (b) the isothermal compressibility of ice II at $T = 237.65$ K predicted by the TIP4P/2005 and TIP4P/Ice models with experimental data reported by Gagnon et al.[52] In (b), the solid line corresponds to the experimental data (ref 52), the dashed line to the results of the TIP4P/2005 model, and the dotted line to the TIP4P/Ice.

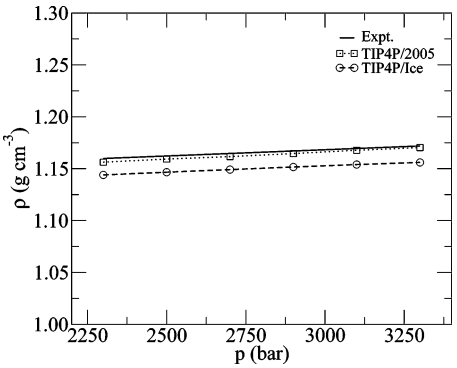

Figure 7. Comparison of the temperature dependence of the density of ice III at $T = 237.65$ K predicted by the TIP4P/2005 and TIP4P/Ice models with experimental data reported by Gagnon et al.[52]

ices II, III, V, and VI, Gagnon et al. measured the pressure dependence of density at $T = 237.65$ K. Gagnon et al. fitted their experimental results to linear or quadratic equations $\rho(p)$.[52,74,75] Finally, the group of Finney and co-workers has also published experimental measurements of the structure and density of D_2O ices II, III, and V for a few thermodynamic states. As before, we will assume that the unit cell of H_2O will not be effected much by the change of the hydrogen isotope.

Figure 5 shows a comparison of our EOS fitted to the TIP4P/Ice and TIP4P/2005 simulations with the experimental results by Fortes et al.[73] for ice II. In both cases, our EOS predicts reasonably well the experimental results along the isotherm $T = 225$ K (see Figure 5b). As for ice Ih, the TIP4P/2005 leads to a slightly better agreement with experiments (within 0.4−0.6%) than that of the TIP4P/Ice model (around 2%). Similarly, the behavior along the isobar at room pressure follows the same trend as that observed for ice Ih (see Figure 5a), that is, the agreement between our EOS and the experiments is good in the high-temperature region (around 150 K), but the deviations become larger as the temperature decreases from this value. This reinforces our belief that quantum effects must be taken into account to perform simulations of ices below $T \approx 150$ K.

Before comparing our results with the experiments of Gagnon et al., there is one issue that should be mentioned. For ice III, there is some ambiguity in the results of Gagnon et al., as these authors report different expressions for the dependence of the density with pressure in refs 52, 74, and 75. The best agreement with our results is obtained with the expression proposed most recently,[74] and hence, this expression will be used to represent the experimental data for ice III (see Figure 7). This ambiguity in the results had already been pointed out by Tchijov et al.,[49] who have also chosen the expression given in ref 74 as the most reliable expression.

Figures 6a, 7, 8, and 9 and Table 4 show a comparison of our results with the experimental data of Gagnon et al. for ices II, III, V, and VI, respectively. As in this case, the experimentally studied states are not always within the region of validity of our EOS; the data shown corresponds to direct results of the simulations, not to results obtained from the proposed EOS (eq 4). For all of these solid phases, the agreement between both models and the experiments is quite good. However, it is generally observed that the TIP4P/2005 model more accurately reproduces the experimental results, in analogy to what happened for ice Ih. The differences between the predictions of the TIP4P/2005 potential and the experimental data are usually between 0.1 and 0.3%, while for the TIP4P/Ice model, they are on the order of 1.0−1.5%. These percentages hold for all of the studied solid phases (including Ih, III, V, and VI), except for ice II, for which the error made by the two models increases appreciably (for ice II, the errors are around 0.6−0.7% for the TIP4P/2005 model and around 1.7−1.9% for the TIP4P/Ice).

Finally, we also compared our results with the experimental measurements of Lobban et al.[63,64] (see Table 5). Again, the same general conclusions as those observed from the comparison with the previous experiments can be inferred. As before, the TIP4P/2005 predictions differ by around 0.2% from experiments and the TIP4P/Ice by about 1.0−1.5%. The error is larger for ice II (0.4% for the TIP4P/2005 and 1.5−2.0% for the TIP4P/Ice).

TABLE 4: Comparison of the Experimental Variation of the Density with Pressure along the Isotherm $T = 237.65$ K for Ices II, III, V, and VI as Obtained by Gagnon et al.[52] with the Simulation Results for the Models TPI4P/Ice and TIP4P/2005, Respectively

		ρ (g cm^{-3})		
ice	p (bar)	expt.	TIP4P/2005	TIP4P/Ice
II	2300	1.1886	1.1811	1.1680
II	2500	1.1903	1.1827	1.1694
II	2700	1.1919	1.1840	1.1706
II	2900	1.1935	1.1855	1.1718
II	3100	1.1952	1.1870	1.1732
II	3300	1.1968	1.1885	1.1744
III	2300	1.1598	1.1563	1.1439
III	2500	1.1622	1.1593	1.1466
III	2700	1.1647	1.1616	1.1491
III	2900	1.1671	1.1646	1.1516
III	3100	1.1695	1.1677	1.1540
III	3300	1.1719	1.1704	1.1560
V	3300	1.2502	1.2518	1.2376
V	3800	1.2561	1.2558	1.2409
V	4300	1.2615	1.2597	1.2444
V	4800	1.2663	1.2632	1.2477
V	5300	1.2706	1.2672	1.2510
V	5800	1.2743	1.2710	1.2545
VI	6400	1.3455	1.3486	1.3317
VI	7000	1.3531	1.3523	1.3350
VI	7500	1.3580	1.3554	1.3378
VI	8000	1.3617	1.3585	1.3405
VI	8500	1.3643	1.3616	1.3433
VI	9000	1.3656	1.3646	1.3460
VI	9500	1.3656	1.3675	1.3486

TABLE 5: Comparison of Experimental Measurements of the Density of Ices II, III, and V Performed by Lobban et al.[63,64] with the Values Given by the TIP4P/2005 and TIP4P/Ice EOSs, Respectively

			ρ (g cm^{-3})		
ice	p (bar)	T (K)	expt.	TIP4P/2005	TIP4P/Ice
II	2800	200.0	1.1980	1.1956	1.1811
II	4200	250.0	1.1948	1.1937	1.1770
II	4800	200.0	1.2147	1.2094	1.1933
III	2500	250.0	1.1540	1.1553	1.1434
III	3000	250.0	1.1621	1.1625	1.1498
III	3300	250.0	1.1649	1.1666	1.1536
V	4000	254.0	1.2533	1.2515	1.2375
V	5000	254.0	1.2631	1.2600	1.2446
V	5000	237.0	1.2680	1.2655	1.2493
V	5000	233.5	1.2594	1.2665	1.2502

C. Thermodynamic Coefficients. The EOS $\rho(p,T)$ served to calculate several thermodynamic coefficients. We chose to compute the isothermal compressibility (κ_T)

$$\kappa_T = \frac{1}{\rho}\left(\frac{\partial \rho}{\partial p}\right)_T \tag{6}$$

the cubic expansion coefficient (α)

$$\alpha = -\frac{1}{\rho}\left(\frac{\partial \rho}{\partial T}\right)_p \tag{7}$$

the pressure coefficient (β)

$$\beta = \left(\frac{\partial p}{\partial T}\right)_V \tag{8}$$

and the heat capacity at constant pressure (C_p)

$$C_p = \left(\frac{\partial H}{\partial T}\right)_p \tag{9}$$

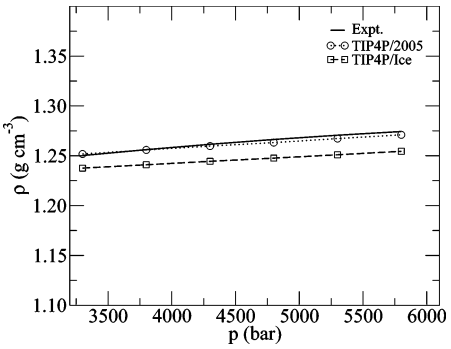

Figure 8. Comparison of the temperature dependence of the density of ice V at $T = 237.65$ K predicted by the TIP4P/2005 and TIP4P/Ice models with experimental data reported by Gagnon et al.[52]

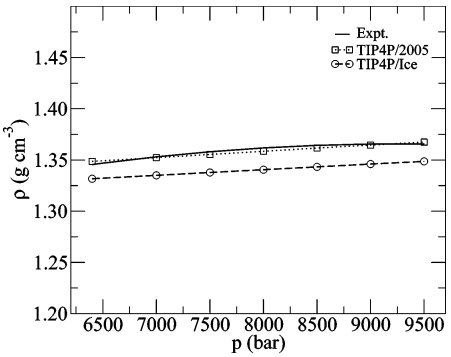

Figure 9. Comparison of the temperature dependence of the density of ice VI at $T = 237.65$ K predicted by the TIP4P/Ice and TIP4P/2005 models with experimental data reported by Gagnon et al.[52]

All of these coefficients have been obtained by derivation of the EOS. In the case of the constant pressure heat capacity C_p, besides the EOS, the internal energy is also needed. The kinetic contribution was calculated using the theorem of the equipartition of the energy (i.e., (3/2)RT due to the translational degrees of freedom plus (3/2)RT due to the rotational), and the potential energy was obtained from the simulations, by fitting the data along an isobar to a polynomial.

Most of these properties have been experimentally measured for ice Ih. Therefore, as we did for the densities, a detailed comparison of the results of the simulations for the TIP4P/Ice and TIP4P/2005 models with the experimental measurements will serve to assess the reliability of the simulations and of the models in predicting these properties.

A comparison of the isothermal compressibility (κ_T) as predicted by our proposed EOS with that obtained from the experimental FW EOS is shown in Figure 10. Our EOS reproduces the isothermal compressibility fairly well, although in this case, the differences with the FW EOS are considerably larger than those found for the density. In particular, for the TIP4P/Ice, the differences are typically on the order of 20−30%. The results of the TIP4P/2005 are only slightly better, again yielding better results at room temperature (10−15% error) than those at low temperatures (20−30% error). Taking into account that the dispersion in the experimental value of κ_T is quite large, with values given by different authors differing by more than 100%, as pointed out by Feistel and Wagner,[48] our results are still reasonable.

On the contrary, the predicted cubic expansion coefficient and the pressure coefficient deviate considerably from the experimental results. At room temperature, the magnitude of α and β predicted by the TIP4P/Ice and TIP4P/2005 EOS are within a 20−30% of the corresponding values as obtained from

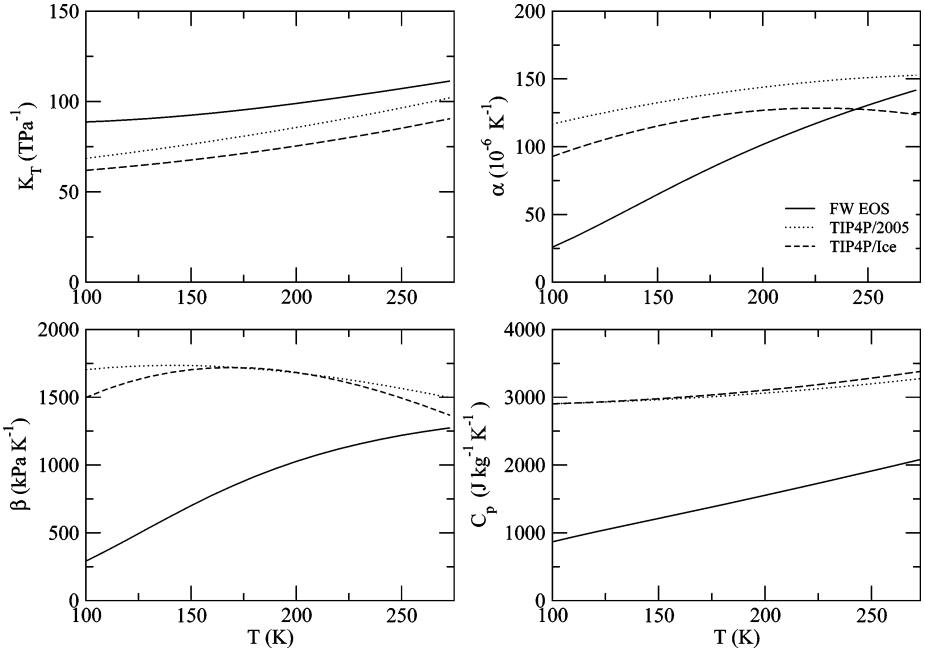

Figure 10. Thermodynamic coefficients (κ_T, α, β, and C_p) for ice Ih at $p = 1000$ bar predicted by the TIP4P/Ice and TIP4P/2005 models. For comparison, the equation of state derived from the experimental-based FW EOS is also shown.

the FW EOS. However, at low temperatures, the differences are as large as 100−200%. These discrepancies between the simulations and the experiments are again a consequence of the classical treatment of the simulations. As mentioned before, according to the third law of thermodynamics, α and β (note that $\beta = \alpha/\kappa_T$) should go to 0 at 0 K.[69] However, classical simulations violate this principle, and the error in these magnitudes become larger at lower temperatures, where quantum effects become more relevant. From these results, we conclude that an estimate of the magnitude of α and β can be obtained at temperatures close to room temperature, while the prediction is not reliable at low temperatures.

The calculated heat capacity is shown in Figure 10. This magnitude is not well reproduced by the simulations. The results differ by at least 50% from experiments, and the largest deviations are found at the lower temperatures. In particular, the heat capacity does not seem to approach 0 as the temperature is decreased, as it also should according to the third law of thermodynamics.[69]

Therefore, from the analysis of the results for ice Ih, it can be concluded that it is possible to obtain reasonable estimations of the isothermal compressibility over the whole range of temperatures from molecular simulations using the TIP4P/Ice and TIP4P/2005 models. Moreover, it is also possible to estimate the order of magnitude of α and β at room temperature. This is an interesting result because for the rest of the ices, there are much less experimental data, and therefore, our EOS provides a first estimate of the thermodynamic properties of ices. Besides, from the analysis of the data for ice Ih, we know up to what extent these predictions are reliable. However, the predictions of C_p are much less reliable.

For the rest of the ices (II, III, V, and VI), a comparison of the predicted isothermal compressibility and the cubic thermal expansion with the data reported by several experimental groups[52,63,64,73] can be found in Table 6. For ice II, we have also plotted the variation of κ_T with pressure along the isotherm $T = 237.65$ K (see Figure 6b). All of these thermodynamic coefficients have been obtained through derivation of the EOS (eq 4), except for the values of κ_T at the thermodynamic states

TABLE 6: Isothermal Compressibility (κ_T) and Thermal Expansion Coefficient (α) for Ices II, III, V, and VI, as Predicted by the TIP4P/2005 and TIP4P/Ice Models, Together with Some Experimental Measurements; κ_T and α were Obtained from the Fit (eq 4), Except for the Values of κ_T at $T = 237.65$ K, Which were Obtained Directly from Simulation Results along That Isotherm (Those Data are Included as Supporting Information)

			κ_T (TPa^{-1})		
ice	p (bar)	T (K)	expt.	TIP4P/2005	TIP4P/Ice
II[a]	3500	200.0	68	57	51
II[b]	3500	225.0	70	60	54
II[c]	2800	237.65	69	62	54
III[c]	2800	237.65	103	121	105
V[c]	4600	237.65	75	61	54
VI[c]	8000	237.65	46	45	41
			α (10^{-6} K^{-1})		
ice	p (bar)	T (K)	expt.	TIP4P/2005	TIP4P/Ice
II[d]	4000	225.0	261 ± 2	231	207
III[d]	2500	245.0	239 ± 12	181	191
V[d]	5000	245.5	240 ± 5	258	223
VI[e]	10540	200.0	33	211	189

[a] From ref 64. [b] From ref 73. [c] From ref 52. [d] From ref 90 quoted by ref 73. [e] From ref 76.

that are compared to the experimental results of Gagnon et al.[52] In that particular case, as some additional simulations have been performed along the $T = 237.65$ K isotherm so that a direct comparison with experiments was possible (see discussion in section IIIB and Figures 6, 7, 8, and 9), the values of κ_T have been obtained by fitting the variation of the density with pressure along this isotherm to a second degree polynomial and deriving it with respect to pressure.

The results shown in Table 6 reinforce some of the conclusions derived from the analysis made for ice Ih. First, the isothermal compressibility κ_T is reasonably well reproduced for all of these ice phases. The deviation from the experiments is about 15% for the TIP4P/2005 model and less than 30% for the TIP4P/Ice potential. Second, the predictions of the cubic thermal expansion α values of both models are within a 10−20% of the experiments. However, in this case, the experimental

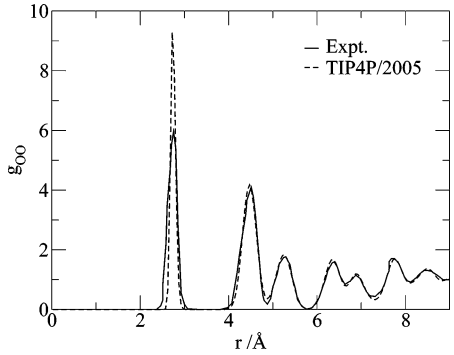

Figure 11. Oxygen−oxygen distribution function of ice Ih at $T = 77$ K and $p = 1$ bar, as obtained from simulations using the TIP4P/2005 model, along with the experimental data given in ref 77.

data are insufficient to assess what model performs the more accurate estimations. Note that for ice VI, the difference with the experimental value is considerably larger than that found for the other ice polymorphs. However, as already pointed out by Shaw,[53] this small experimental value of α[76] might not be very reliable, as it might be effected by an anomaly in α between 100−200 K, and that was attributed to an order−disorder transition.

D. Structure of Ices. In the previous sections, we have seen that the TIP4P/2005 model is able to predict the experimental EOS of ices Ih, II, III, V, and VI with good accuracy. It would be interesting to check if this model is also able to reproduce the correct structure of the ice phases. For that purpose, we have computed the oxygen−oxygen radial distribution function of ice Ih at 77 K and 1 bar, which has also been estimated experimentally.[77] In this case, the simulations were performed in a simulation box containing 432 molecules so that the radial distribution function could be safely evaluated up to 9 Å. It can be seen in Figure 11 that the agreement between simulations and theory is good, the main difference being that the TIP4P/2005 model predicts a higher and slightly narrower first peak. These discrepancies are probably also due to quantum effects that have not been taken into account in our simulations. The good agreement with the experimental results found for ice Ih gives us confidence that the radial distribution functions for the other ice polymorphs (which, to the best of our knowledge, have not yet been experimentally obtained[78]) are also probably correct, at least quantitatively. The $g(r)$ for ices Ih, II, III, V, and VI for the TIP4P/2005 model at some thermodynamic states are given as Supporting Information.

E. Revision of the Densities of Ice Polymorphs. When testing the performance of the different water potentials to describe the densities of the solid phases of water, it has become popular to use one thermodynamic state per ice.[26,45,46] The selected states are those reported in the book of Petrenko and Whitworth.[2] Those data are shown in Table 7. Now that we have estimated up to what temperatures our classical simulations yield reliable results, it is interesting to go over these data again and to analyze the possible origin of the discrepancies. For completeness, the densities of the two recently discovered ice polymorphs, that is, ice XIII and ice XIV,[8,56] have also been included in Table 7.

A careful look at Table 7 shows that the ices for which the discrepancies between simulation and experiment are larger are precisely those for which the comparison is made at temperatures around or below 100 K, namely, ice Ic, IV, VIII, XI, XIII, and XIV. Besides, the differences for ices Ic, XI, and XIII are on the same order of magnitude as those observed for ice Ih at low temperatures (see Table 3). This suggests that probably these

TABLE 7: Densities (g cm^{-3}) of Several Ice Forms[a]

ice	T (K)	p (bar)	TIP4P/2005	expt.
Ih	250	0	0.921	0.920
Ic	78	0	0.944	0.931*
II	123	0	1.199	1.170[b] 1.190[c]
III	250	2800	1.160	1.165
IV	110	0	1.293	1.272*
IV	260	5000	1.280	1.290[d]
V	223	5300	1.272	1.283
VI	225	11000	1.380	1.373
VIII	10	24000	1.634	1.628*
IX	165	2800	1.190	1.194
XI	5	0	0.954	0.934*
XII	260	5000	1.296	1.292
XIII	80	1	1.251	1.244*
XIV	80	1	1.294	1.332*

[a] Experimental data were taken from ref 2, and for completeness, the densities of the two recently discovered ices (ice XIII and ice XIV) have also been included.[8,56] We have marked those data corresponding to low-temperature states and which are not likely to be correctly predicted by classical simulations with an asterisk. For ice IV, a higher temperature was included so that a comparison is possible in a region where quantum effects are not as important, and for Ice II, a new experimental measurement was added on the right column. [b] From ref 79. [c] From ref 73. [d] From ref 7.

discrepancies are due to quantum effects, which are not included in the classical simulations of this work. If there were experimental data available for all ice polymorphs at temperatures above 150 K, these two models would most likely exhibit an improved performance. Indeed, for ice IV, it can be seen that the experimental density is more accurately reproduced at the state $T = 260$ K and $p = 5000$ bar than at the state $T = 110$ K and $p = 0$ bar (see Table 7). Thus, Table 7 shows that the ability of the TIP4P/2005 model to describe Ih and Ic is probably quite similar, and the largest deviation found for ice Ic is just a consequence of the low temperature selected for this ice. One could argue that quantum effects are also present at room temperature, where the simulations appear to lead to results very close to experiments. We would like to stress that the parameters of these potentials have been fitted to reproduce some properties of water at room temperature, and therefore, quantum effects are implicitly included in the parametrization of the potential. As the temperature is decreased, quantum effects become larger, and the potentials are no longer valid. This does not mean that these are bad potentials, but it exemplifies that quantum corrections are important and must be included in the simulations in order to reproduce the behavior of ices at low temperatures (i.e., below 100−150 K).

For the ices IV and VIII, the differences with experimental data are not similar to those found for ice Ih. For ice IV, the difference is somewhat larger than that found for ice Ih at $T =$ 100 K, while for ice VIII, the prediction of the TIP4P/2005 model is surprisingly in quite good agreement with the experimental result ($\Delta\rho = 0.003$ versus $\Delta\rho \approx 0.02$ found for ice Ih at this same temperature, i.e., $T = 10$ K). These suggest that other effects might also be present or, perhaps, that quantum corrections might not have the same magnitude for all ice polymorphs. In particular, for ice VIII, there might be a cancellation between several effects. Indeed, our results show that either the TIP4P/2005 and the TIP4P/Ice models tend to underestimate the isothermal compressibility κ_T for most of the ice polymorphs (see Figures 6b and 10 and Table 6). For ice VIII, the comparison between simulation and experiment is made at a quite high pressure state (24000 bar). Assuming that, in analogy with the results found for other ice polymorphs, the TIP4P/2005 model underestimates the value of κ_T, this will result

TABLE 8: Residual Energies and Densities of the Ices at Zero Temperature and Pressure Predicted by the TIP4P/2005 and TIP4P/Ice Models

	TIP4P/2005		TIP4P/Ice	
phase	U (kcal mol^{-1})	ρ (g cm^{-3})	U (kcal mol^{-1})	ρ (g cm^{-3})
Ih	−15.059	0.9538	−16.465	0.938
II	−14.847	1.2301	−16.268	1.212
III	−14.741	1.1838	−16.140	1.169
V	−14.644	1.2971	−16.049	1.277
VI	−14.513	1.3851	−15.917	1.363

in an underestimation of the density of ice VIII at this high pressure, which is precisely the opposite effect to that caused by the quantum corrections. Therefore, it is possible that a cancellation between the two effects had occurred.

The case of ice II deserves a separate discussion. The simulations of ice II at 123 K and 0 MPa exhibit the largest discrepancy with the experimental result of Kamb (i.e., $\rho = 1.170$ g cm^{-3}),[79] for both the TIP4P/Ice and TIP4P/2005 potential models.[45,46] However, this is not a particularity of these two potentials. This large discrepancy with the experimental datum for ice II seems to be the general rule for most of the models of water. In view of this, even though it is a quite low temperature state (123 K), the error is less likely to be due only to the classical treatment of the simulations.[45] In fact, more recent neutron diffraction experiments suggest that the use of helium gas as a medium for applying pressure might have some consequences on the measured structure as helium atoms are able to enter in the open channels of ice II.[64,73,80] This effect has also been studied by means of ab initio calculations.[81] Indeed, when we compare the results of the simulations with some recent experimental measurements that used argon instead of helium for applying the pressure, the agreement between the simulations and experiments is quite good (see Table 7 and Figure 5a). This would explain why none of the potential models seemed to be able to reproduce the experimental density of ice II. One is tempted to suggest that for $T > 150$ K, a deviation from the predictions of the TIP4P/2005 potential by about 1.5% or larger may certainly suggest some error in the experimental measurement. With this is mind, it is now simple to see that the density of ice II of Kamb[79] was wrong and that the new value of Fortes et al. seems more appropriate.[73] It is worth mentioning that Whalley also pointed out some inconsistency between the measurement of Kamb and his own measurement of the volume of ice II while studying the properties of ices at zero temperature and pressure.[82]

F. Zero Temperature Properties. For completeness, we have also evaluated some of the properties of the TIP4P/Ice and TIP4P/2005 models at zero temperature and pressure. That was done for the different ice phases considered in this work. To obtain the zero temperature properties, consecutive Parrinello−Rahman NpT simulations at $p = 0$ bar and between 40 and 1 K were performed. The configurational energy and density exhibit linear behavior in this range of temperature, and hence, the properties at zero temperature were obtained from a simple linear extrapolation. An estimate of the energy under these conditions has been done by Whalley, who used measurements of the volume at 90 K, along with some previous estimates of the coexistence lines between the different ice phases, to obtain an extrapolated value of the energy at zero temperature and pressure.[82] The configurational internal energy and density at zero pressure and temperature for all of the studied ice phases are shown in Table 8. Both models predict that ice Ih is the most stable phase at these conditions (i.e., the one with the minimum internal energy), which is in keeping with experimental results.[82]

TABLE 9: Relative Energy of the Ices with Respect to Ice II at Zero Temperature and Pressure Predicted by the TIP4P/2005 and TIP4P/Ice Models; for Comparison, the Experimental Measurements of Whalley are also Included[82]

	ΔU (kcal mol^{-1})		
phase	TIP4P/Ice	TIP4P/2005	expt.
Ih	−0.197	−0.212	−0.014
II	0	0	0
III	0.128	0.106	0.201
V	0.219	0.203	0.213
VI	0.351	0.344	0.373

The relative energies with respect to ice II have also been computed as this allows a comparison with the experimental results of Whalley[82] (see Table 9). As it can be seen in the table, both models correctly predict the order of the internal energies of the ices Ih, II, III, V, and VI, the internal energy increasing in this order. Besides, the simulations reproduce the order of magnitude of the differences between the energies of ices III, V, VI, and that of ice II fairly well. The main discrepancy is the value of the energy of ice Ih with respect to that of ice II. For both TIP4P/Ice and TIP4P/2005 models, ice I_h is much more stable than ice II at 0 K. However, according to the experimental results, ice Ih is only slightly more stable than ice II under these circumstances. Further work is needed to determine the origin of this discrepancy. Taking into account that the differences in internal energies at 0 K are quite small (on the order of 0.3 kcal/mol), it can be stated that the predictions of the TIP4P/Ice and TIP4P/2005 models appear as quite reasonable. Although quantum effects are of course quite important at 0 K (and that may cast some doubts on our results), it seems that classical simulations can still be useful to estimate the energy difference between ices at 0 K, provided that the vibrational zero point energies are similar for the different ice polymorphs.

IV. Conclusions

In this paper, we propose an EOS for five of the thermodynamically stable solid phases of water, including ices Ih, II, III, V, and VI. For each ice, the nine parameters of the EOS have been fitted to the results of MC simulations using the TIP4P/2005 and TIP4P/Ice models for a large number of thermodynamic states within the experimental region where each phase is thermodynamically stable. From this EOS, several thermodynamic coefficients have been calculated, namely, the isothermal compressibility, the cubic thermal expansion, the pressure coefficient, and the heat capacity at constant pressure.

A detailed comparison with the available experimental data for ice Ih let us to infer some interesting conclusions. First, the density is accurately reproduced by both models as long as the temperature is above around 150 K. With regards to the thermodynamic coefficients, the isothermal compressibility κ_T is also reasonably well reproduced by the two models at temperatures close to room temperature, although, in this case, the discrepancies with experiments are as large as 20%. Previous work has shown that the TIP4P/2005 model is also able to reproduce the experimental isothermal compressibility of water at room temperature and pressure more accurately than other similar models. The TIP4P/2005 model predicts $\kappa_T = 46.5 \times 10^{-5}$ MPa^{-1},[45] to be compared with the experimental value $\kappa_T = 45.8 \times 10^{-5}$ MPa^{-1} and with the predictions of the TIP4P, $\kappa_T = 59 \times 10^{-5}$ MPa^{-1}, and TIP5P models, $\kappa_T = 40.5 \times 10^{-5}$ MPa^{-1}.[83] Simulations also provide an estimate of the order of magnitude of the parameters α and β, whereas the prediction

of C_p is not very reliable. Second, the TIP4P/2005 model systematically shows a slightly better agreement with experiments than the TIP4P/Ice. Third, the deviations of all of these magnitudes are larger at low temperatures. As expected, quantum effects become more important in the low-temperature region. As a consequence of the classical treatment, neither the thermal expansion, the pressure coefficient, nor the heat capacity approach zero at zero temperature, as they should according to the third law of thermodynamics. Therefore, the simulations performed here have allowed us to establish a lower limit in the temperature, that is, $T = 150$ K, beyond which classical simulations are not valid.

For the rest of the ices, there are less experimental data available, and therefore, our simulations provide a first estimate of the thermodynamic properties over the whole range of thermodynamic stability. Besides, from the analysis made for ice Ih, we know up to what extent these predictions are reliable. Moreover, in the instances where experimental measurements are available, the deviations of simulations from experiments seems to follow the same trend as that observed for ice Ih.

Besides properly describing the crystalline phases of water, recent works have shown that the TIP4P/2005 model is also able to reproduce the properties of methane hydrates.[84,85] However, the TIP4P/2005 model is not only a model to describe solid phases. It has been shown that this model is also able to describe properly the liquid−vapor equilibrium[86,87] and the surface tension of water.[88]

The reason why the TIP4P/2005 model reproduces the experimental data better than the TIP4P/Ice model is probably because trying to reproduce the melting temperature of ice Ih with a nonpolarizable model (as is the case of the TIP4P/Ice model) can only be achieved at the expense of lowering the predicted densities of the ice polymorphs.

The TIP4P/2005 model has also been shown to reproduce the structure of ices to good accuracy. In particular, the simulated oxygen−oxygen radial distribution function for ice Ih at 77 K and 1 bar is in very good agreement with the experimental measurements,[77] except that the TIP4P/2005 model overestimates the height of the first peak.

Finally, the properties at zero temperature and pressure have also been estimated. The simulated relative energies of these ice polymorphs agree quite well with the experimental results, predicting the right ordering in energies, namely, ice Ih, II, III, V, and VI.[82] The main discrepancy between simulations and theory is the difference of energies between ice Ih and II, which seems to be largely overestimated by the simulations. Further work is needed to understand the origin of this discrepancy.

In summary, the results provided here represent what probably can be best achieved to describe ices using a rigid, nonpolarizable model within a classical treatment, and an improvement can probably only be made by using a potential model that includes polarizability[89] and by performing simulations that take into account quantum effects.

Acknowledgment. This work was funded by Grants FIS2007-66079-C02-01 from the Dirección General de Investigación, S-0505/ESP/0229 from the CAM, MTKD−CT-2004-509249 from the European Union, and 910570 from the UCM. E.G.N. wishes to thank the Ministerio de Educación y Ciencia and the Universidad Complutense de Madrid for a Juan de la Cierva fellowship. C.M. performed part of this work during a stay in the Technical University of Berlin, funded by the "Ayuda para Profesores" programme of the UCM. We would like to thank Professor Pedro Sanz, Professor J. L. Abascal, Professor L. G. MacDowell, and Professor B. Slater for useful discussions and Professor Eduardo Sanz for providing us the data from the plot of the experimental radial distribution function given in ref 77.

Supporting Information Available: Density and residual energy for all states within the region of thermodynamic stability, density and energy along the 100 K isotherm, and structural pair correlation functions between oxygen−oxygen, hydrogen−hydrogen, and oxygen−hydrogen for ices Ih, II, III, V, and VI. This material is available free of charge via the Internet at http://pubs.acs.org.

References and Notes

(1) Eisenberg, D.; Kauzmann, W. *The Structure and Properties of Water*; Oxford University Press: London, 1969.
(2) Petrenko, V. F.; Whitworth, R. W. *Physics of Ice*; Oxford University Press: London, 1999.
(3) Chaplin, M. Water Structure and Science. http://www.lsbu.ac.uk/water/ (2005).
(4) Finney, J. L. *Philos. Trans. R. Soc. London, Ser. B* **2004**, *359*, 1145.
(5) Tammann, G. *Kristallisieren und Schmelzen*; Johann Ambrosius Barth: Leipzig, Germany, 1903.
(6) Bridgman, P. W. *Proc. Am. Acad. Sci. Arts* **1912**, *47*, 441.
(7) Lobban, C.; Finney, J. L.; Kuhs, W. F. *Nature* **1998**, *391*, 268.
(8) Salzmann, C. G.; Radaelli, P. G.; Hallbrucker, A.; Mayer, E.; Finney, J. L. *Science* **2006**, *311*, 1758.
(9) Venkatesh, C. G.; Rice, S. A.; Narten, A. H. *Science* **1974**, *186*, 927.
(10) Debenedetti, P. G. *J. Phys.: Condens. Matter* **2003**, *15*, R1669.
(11) Mishima, O.; Calvert, L. D.; Whalley, E. *Nature* **1984**, *310*, 393.
(12) Mishima, O.; Stanley, H. E. *Nature* **1998**, *396*, 329.
(13) Poole, P. H.; Sciortino, F.; Essmann, U.; Stanley, H. E. *Nature* **1992**, *360*, 324.
(14) Suter, M. T.; Andersson, P. U.; Petterson, J. B. C. *J. Chem. Phys.* **2006**, *125*, 174704.
(15) Barker, J. A.; Watts, R. O. *Chem. Phys. Lett.* **1969**, *3*, 144.
(16) Rahman, A.; Stillinger, F. H. *J. Chem. Phys.* **1971**, *55*, 3336.
(17) Guillot, B. J. *Mol. Liq.* **2002**, *101*, 219.
(18) Jorgensen, W. L.; Chandrasekhar, J.; Madura, J. D.; Impey, R. W.; Klein, M. L. *J. Chem. Phys.* **1983**, *79*, 926.
(19) Berendsen, H. J. C.; Postma, J. P. M.; van Gunsteren, W. F.; Hermans, J. *Intermolecular Forces*; Pullman, B, Ed.; Reidel: Dordrecht, The Netherlands, 1982; p 331.
(20) Berendsen, H. J. C.; Grigera, J. R.; Straatsma, T. P. *J. Phys. Chem.* **1987**, *91*, 6269.
(21) Mahoney, M. W.; Jorgensen, W. L. *J. Chem. Phys.* **2000**, *112*, 8910.
(22) Rahman, A.; Stillinger, F. H. *J. Chem. Phys.* **1972**, *57*, 4009.
(23) Morse, M. D.; Rice, S. A. *J. Chem. Phys.* **1982**, *76*, 650.
(24) Ayala, R. B.; Tchijov, V. *Can. J. Phys.* **2003**, *81*, 11.
(25) Rick, S. W. *J. Chem. Phys.* **2005**, *122*, 094504.
(26) Baranyai, A.; Bartók, A.; Chialvo, A. A. *J. Chem. Phys.* **2005**, *123*, 54502.
(27) Otero, L.; Molina-Garcia, A. D.; Sanz, P. D. *Crit. Rev. Food Sci. Nutr.* **2002**, *42*, 339.
(28) Carignano, M. A.; Shepson, P. B.; Szleifer, I. *Mol. Phys.* **2005**, *103*, 2957.
(29) Slovak, J.; Tanaka, H. *J. Chem. Phys.* **2005**, *122*, 204512.
(30) Picaud, S. *J. Chem. Phys.* **2006**, *125*, 174712.
(31) Koyama, Y.; Tanaka, H.; Gao, G.; Zeng, X. C. *J. Chem. Phys.* **2004**, *121*, 7926.
(32) Buch, V.; Martoňák, R.; Parrinello, M. *J. Chem. Phys.* **2006**, *124*, 204705.
(33) Tribello, G. A.; Slater, B.; Salzmann, C. G. *J. Am. Chem. Soc.* **2006**, *128*, 12594.
(34) Sanz, E.; Vega, C.; Abascal, J. L. F.; MacDowell, L. G. *Phys. Rev. Lett.* **2004**, *92*, 255701.
(35) Sanz, E.; Vega, C.; Abascal, J. L. F.; MacDowell, L. G. *J. Chem. Phys.* **2004**, *121*, 1165.
(36) MacDowell, L. G.; Sanz, E.; Vega, C.; Abascal, L. F. *J. Chem. Phys.* **2004**, *121*, 10145.
(37) McBride, C.; Vega, C.; Sanz, E.; Abascal, J. L. F. *J. Chem. Phys.* **2004**, *121*, 11907.
(38) McBride, C.; Vega, C.; Sanz, E.; MacDowell, L. G.; Abascal, J. L. F. *Mol. Phys.* **2005**, *103*, 1.
(39) Vega, C.; McBride, C.; Sanz, E.; Abascal, J. L. *Phys. Chem. Chem. Phys.* **2005**, *7*, 1450.
(40) Vega, C.; Sanz, E.; Abascal, J. L. F. *J. Chem. Phys.* **2005**, *122*, 114507.

(41) Vega, C.; Abascal, J. L. F.; Sanz, E.; MacDowell, L. G.; McBride, C. *J. Phys.: Condens. Matter* **2005**, *17*, S3283.
(42) Bernal, J. D.; Fowler, R. H. *J. Chem. Phys.* **1933**, *1*, 515.
(43) Fernandez, R. G.; Abascal, J. L. F.; Vega, C. *J. Chem. Phys.* **2006**, *124*, 144506.
(44) Horn, H. W.; Swope, W. C.; Pitera, J. W.; Madura, J. D.; Dick, T. J.; Hura, G. L.; Head-Gordon, T. *J. Chem. Phys.* **2004**, *120*, 9665.
(45) Abascal, J. L. F.; Vega, C. *J. Chem. Phys.* **2005**, *123*, 234505.
(46) Abascal, J. L. F.; Sanz, E.; Fernández, R. G.; Vega, C. *J. Chem. Phys.* **2005**, *122*, 234511.
(47) Vega, C.; Abascal, J. L. F. *J. Chem. Phys.* **2005**, *123*, 144504.
(48) Feistel, R.; Wagner, W. *J. Phys. Chem. Ref. Data* **2006**, *35*, 1021.
(49) Tchijov, V.; Ayala, R. B.; Len, G. C.; Nagornov, O. *J. Phys. Chem. Solids* **2004**, *65*, 1277.
(50) Len, G. C.; Romo, S. R.; Tchijov, V. *J. Phys. Chem. Solids* **2002**, *63*, 843.
(51) Fei, Y.; Mao, K. H.; Hemley, R. J. *J. Chem. Phys.* **1993**, *99*, 5369.
(52) Gagnon, R. E.; Kiefte, H.; Clouter, M. J.; Whalley, E. *J. Chem. Phys.* **1990**, *92*, 1909.
(53) Shaw, G. H. *J. Chem. Phys.* **1986**, *84*, 5862.
(54) Báez, L. A.; Clancy, P. *J. Chem. Phys.* **1995**, *103*, 9744.
(55) Gao, G. T.; Zeng, X. C.; Tanaka, H. *J. Chem. Phys.* **2000**, *112*, 8534.
(56) Vega, C.; Martin-Conde, M.; Patrykiejew, A. *Mol. Phys.* **2006**, *104*, 3583.
(57) Allen, M. P.; Tildesley, D. J. *Computer Simulation of Liquids*; Oxford University Press: London, 1987.
(58) Frenkel, D.; Smit, B. *Understanding Molecular Simulation*; Academic Press: London, 1996.
(59) Parrinello, M.; Rahman, A. *J. Appl. Phys.* **1981**, *52*, 7182.
(60) Yashonath, S.; Rao, C. N. R. *Mol. Phys.* **1985**, *54*, 245.
(61) Buch, V.; Sandler, P.; Sadlej, J. *J. Phys. Chem. B* **1998**, *102*, 8641.
(62) Pauling, L. *J. Am. Chem. Soc.* **1935**, *57*, 2680.
(63) Lobban, C.; Finney, J. L.; Kuhs, W. F. *J. Chem. Phys.* **2000**, *112*, 7169.
(64) Lobban, C.; Finney, J. L.; Kuhs, W. F. *J. Chem. Phys.* **2002**, *117*, 3928.
(65) McBride, C.; Vega, C.; Sanz, E.; MacDowell, L. G.; Abascal, J. L. F. *Mol. Phys.* **2005**, *1*, 103.
(66) Iglev, H.; Schmeisser, M.; Simeonidis, K.; Thaller, A.; Laubereau, A. *Nature* **2006**, *439*, 183.
(67) Murnaghan, F. *Proc. Natl. Acad. Sci. U.S.A.* **1944**, *30*, 244.
(68) Strässle, T.; Klotz, S.; Loveday, J. S.; Braden, M. *J. Phys.: Condens. Matter* **2005**, *17*, S3029.
(69) Callen, H. B. *Thermodynamics and an Introduction to Thermostatistics*; John Wiley & Sons: New York, 1985.
(70) de la Peña, L. H.; Kusalik, P. G. *J. Chem. Phys.* **2005**, *123*, 144506.
(71) de la Peña, L. H.; Kusalik, P. G. *J. Chem. Phys.* **2006**, *125*, 054512.
(72) Poulsen, J. A.; Nyman, G.; Rossky, P. J. *Proc. Natl. Acad. Sci. U.S.A.* **2005**, *102*, 6709.
(73) Fortes, A. D.; Wood, I. G.; Alfredsson, M.; Vočadlo, L.; Knight, K. S. *J. Appl. Crystallogr.* **2005**, *38*, 612.
(74) Tulk, C. A.; Gagnon, R. E.; Kiefte, H.; Clouter, M. J. *J. Chem. Phys.* **1997**, *107*, 10684.
(75) Tulk, C. A.; Gagnon, R. E.; Clouter, M. J. *J. Chem. Phys.* **1994**, *101*, 2350.
(76) Mishima, O.; Mori, N.; Endo, S. *J. Chem. Phys.* **1979**, *70*, 2037.
(77) Narten, A. H.; Venkatesh, C. G.; Rice, S. A. *J. Chem. Phys.* **1976**, *64*, 1106.
(78) Loveday, J. S.; Nelmes, R. J.; Marshall, W. G.; Besson, J. M.; Koltz, S.; Hamel, G. *Physica B* **1998**, *240*, 241.
(79) Kamb, B. *Acta Crystallogr.* **1964**, *17*, 1437.
(80) Arnold, G. P.; Wenzel, R. G.; Rabideau, S. W.; Nereson, N. G.; Bowman, A. L. *J. Chem. Phys.* **1971**, *55*, 589.
(81) Fortes, A. D.; Wood, I. G.; Brodholt, J. P.; Vočadlo, L. *J. Chem. Phys.* **2003**, *119*, 4567.
(82) Whalley, E. *J. Chem. Phys.* **1984**, *81*, 4087.
(83) Jorgensen, W. L.; Tirado-Rives, J. *Proc. Am. Acad. Sci. Arts* **2005**, *102*, 6665.
(84) Docherty, H.; Galindo, A.; Vega, C.; Sanz, E. *J. Chem. Phys.* **2006**, *125*, 074510.
(85) Wierzchowski, S. J.; Monson, P. A. *J. Phys. Chem. B* **2007**, *111*, 7242.
(86) Vega, C.; Abascal, J. L. F.; Nezbeda, I. *J. Chem. Phys.* **2006**, *125*, 034503.
(87) Chialvo, A. A.; Bartók, A.; Baranyai, A. *J. Mol. Liq.* **2006**, *129*, 120.
(88) Vega, C.; de Miguel, E. *J. Chem. Phys.* **2007**, *126*, 154707.
(89) Baranyai, A.; Bartók, A. *J. Chem. Phys.* **2007**, *126*, 184508.
(90) Lobban, C. Ph.D. Thesis, University of London, 1998.